

Stability of Periodically Driven Topological Phases against Disorder

Oles Shtanko¹ and Ramis Movassagh²

¹*Physics Department, Massachusetts Institute of Technology, Cambridge, Massachusetts 02139, USA*

²*IBM Research, MIT-IBM A.I. Lab, 75 Binney Street, Cambridge, MA 02142*

In recent experiments, time-dependent periodic fields are used to create exotic topological phases of matter with potential applications ranging from quantum transport to quantum computing. These nonequilibrium states, at high driving frequencies, exhibit the quintessential robustness against local disorder similar to equilibrium topological phases. However, proving the existence of such topological phases in a general setting is an open problem. We propose a universal effective theory that leverages on modern free probability theory and ideas in random matrices to analytically predict the existence of the topological phase for finite driving frequencies and across a range of disorder. We find that, depending on the strength of disorder, such systems may be topological or trivial and that there is a transition between the two. In particular, the theory predicts the critical point for the transition between the two phases and provides the critical exponents. We corroborate our results by comparing them to exact diagonalizations for driven-disordered 1D Kitaev chain and 2D Bernevig-Hughes-Zhang models and find excellent agreement. This Letter may guide the experimental efforts for exploring topological phases.

The dynamics of nonequilibrium quantum systems has been a subject of active and recent study with experiments involving several dozens of qubits [1, 2]. A promising technique for creating nonconventional states of matter is by the application of a time-periodic field (e.g., to interacting cold atoms). These nonequilibrium states of matter are frequently referred to as *Floquet* phases [3, 4]. The propositions and realizations include Floquet topological insulators [5–10], anomalous Floquet-Anderson insulators [11–13], discrete time crystals [14, 15] etc. Remarkably, the controlled periodic driving helps create Majorana modes with non-Abelian braiding statistics potentially useful in topological quantum computation [16–18].

Local disorder is inevitable in realizing such nonequilibrium phases. Yet engineered systems can utilize artificial disorder as a tool for control [12, 15]. For example, disorder leads to many-body localization [19, 20] preventing uncontrolled heating [14, 21] and stabilizing topological phases of matter [22–25]. Disorder is also responsible for phase transitions [26–30]. Even though topological phases in equilibrium are universally robust against disorder, their Floquet counterparts may not be. In low-dimensional systems, the stability is typically granted by the Anderson localization preserving the bulk mobility gap, even if the disorder closes the bulk spectral gap [31, 32]. The same mechanism protects Floquet topological phases at high frequencies [33]. However, if the driving frequency is finite, Anderson localization may break down depending on the driving amplitude and disorder strength [34–37]. In this regime, nothing can preserve the topological phase if the bulk spectral gap is closed by disorder.

Despite the numerical frontiers [26, 27, 33], it is very difficult to quantify disordered Floquet systems in general. Even though in the limits of high driving frequency and weak disorder one can use techniques such as pertur-

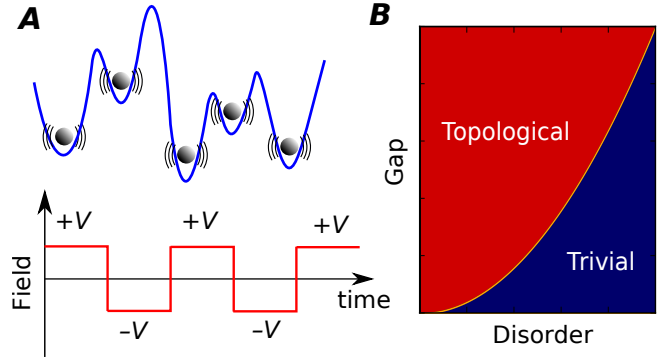


FIG. 1. **Schematics.** **A** An isolated disordered quantum system represented by trapped cold atoms. The time periodic field $V(t)$ induces a transition from a trivial to a topological phase. **B** The phase diagram for the system in the presence of local disorder. An increase of the disorder strength W induces a phase transition at $W_c \sim \Delta_0^{1/2}$, where Δ_0 is the gap of the clean system.

bation theory, many current realizations operate outside these limits [14, 16, 17]. This raises the following questions: Are Floquet topological phases preserved under finite frequency and strong disorder? And if there is a disorder-induced transition into a trivial phase, can one quantify the critical point in the thermodynamic limit?

In this Letter, we leverage on modern free probability theory and ideas inspired by random matrices to answer these questions. The local disorder in the Hamiltonian introduces a correction to the Floquet Hamiltonian (Eq. (2)). At finite driving frequencies, this correction is the sum of (potentially infinitely) many noncommuting terms in the Magnus expansion. Due to its nonlocality and randomness, we find that this correction has level statistics very similar to the Gaussian orthogonal (GOE) or unitary (GUE) ensembles depending on the problem

(Figs. 2 A and B). We propose an effective model for the disordered Floquet Hamiltonian, in which the correction is replaced by a single generic random matrix proportional to the strength of disorder (Eq. (4)). We use free probability theory to analytically demonstrate that the effective Floquet Hamiltonian does indeed exhibit a topological phase at a finite strength of disorder and finite driving frequency. We also find a critical strength of disorder beyond which the spectral gap closes. Consequently, a transition is induced from a topological to a trivial metallic phase. The resulting phase diagram is shown in Fig. 1B. We compare the universal analytical results against exact diagonalization for the disordered Kitaev chain and the 2D Bernevig- Hughes-Zhang (BHZ) model (see Fig. 3).

Consider the problem of noninteracting particles on a lattice. It is useful to divide the Hamiltonian into three parts: the translationally invariant static part H_0 , the static local disorder δV , and the applied external time-periodic driving field $V(t)$ (Fig. 1A). Therefore,

$$H(t) = H_0 + \delta V + V(t), \quad V(t) = V(t + \tau), \quad (1)$$

where τ is the driving period. Since topological phases in the integer quantum Hall universality class are often understood in terms of free particles, we leave the effects of many-body interactions for future work.

Let us first focus on the clean system. By the Floquet-Bloch theorem, the total time evolution at discrete times $t = n\tau$ is given by the unitary operator $U_n = (U_F)^n$, where $U_F \equiv \exp(-i\tau H_F) = \mathcal{T} \exp\left(-i \int_0^\tau dt' H(t')\right)$, \mathcal{T} denotes chronological time ordering, and H_F is the Floquet Hamiltonian. The Hamiltonian H_F defines a new quantum (Floquet) phase [22]. Depending on the field $V(t)$, this phase can be equivalent to the initial phase of H_0 , or be different. Here we focus on the latter case where the field $V(t)$ is designed to convert a trivial into a topological phase [3, 38].

Next we look at the role of disorder, δV , which may be represented by a diagonal random matrix. Periodic driving $V(t)$ and δV dress the bare Floquet Hamiltonian into a disordered Floquet Hamiltonian H'_F defined by

$$H'_F = H_F + \delta V_F, \quad (2)$$

where $\delta V_F \equiv \sum_{\ell \geq 1} \delta V_\ell \tau^{\ell-1}$ with the coefficients

$$\delta V_1 = \delta V, \quad \delta V_\ell = \frac{1}{\tau^\ell} \left[K_\ell \{H(t) + \delta V\} - K_\ell \{H(t)\} \right], \quad (3)$$

denoting by $\{.\}$ a functional. K_ℓ is the ℓ th term in the Magnus expansion (Ref. [3] and the Supplemental Material). In contrast to the random on-site potential δV , in principle, each δV_ℓ contributes nonzero off-diagonal entries to the matrix δV_F , making the effective disorder nonlocal.

If the high driving frequency limit $\Omega = 2\pi/\tau \rightarrow \infty$, the higher-order corrections can be neglected. As a result,

δV_F acts similarly to the local disorder δV , leading to the localization of eigenstates. In this situation, $H_F + \delta V_F$ always describes the topological phase as soon as a mobility gap is present in the system.

On the other hand, if Ω is finite, the higher order terms in Eq.(3) cannot be ignored as τ may exceed the radius of convergence of Eq.(3). Consequently, the off-diagonal entries in δV_F are not negligible. Physically, this corresponds to emergence of driving-induced Landau-Zener transitions between localized states responsible for the breakdown of Anderson localization. In this regime, if the spectral gap closes, the Floquet topological phase is breaking with following disorder-induced transition to a trivial phase.

In general, obtaining the exact spectral properties of Eq. (2) analytically is formidably difficult, mainly limited by the noncommutativity. Further numerical simulations are limited for large system sizes. However, there are many nondiagonal corrections appearing in Eq. (3); the disorder δV added to $H(t)$ smears all over the effective Floquet Hamiltonian (i.e., δV_F in Eq. (2)). It then seems plausible to assume that the resulting δV_F should mimic a generic Hermitian random matrix. Indeed, in Figs. 2 A and B, we show the accuracy by which the level statistics of δV_F are represented by the standard Gaussian ensembles. We will return to this below.

Therefore, the *effective Hamiltonian* we propose is:

$$H_F^{\text{eff}} = H_F + \lambda M, \quad (4)$$

where the matrix M is chosen from the Gaussian ensemble with eigenvalues in $[-2, 2]$, which in the limit of infinite size would follow the semicircle law [39], and $\lambda = \sqrt{\varphi(\delta V_F^2)}$ with $\varphi(A) = \mathbb{E} \text{Tr}(A)/\text{dim}(A)$ denoting the empirical mean of the matrix A . Physically, H_F^{eff} describes a competition between the topological phase ($\lambda < \lambda_c$) and featureless chaotic phase ($\lambda > \lambda_c$), where λ_c is a critical point. This model describes the transitions in a finite range of disorder strength and may not retain the precision in the limit of high disorder $W \gg \Omega$ in which the target Floquet Hamiltonian is expected to exhibit Poissonian quasienergy level statistics.

The value of the parameter λ depends on both disorder strength W and driving period τ (see Supplemental Material for details). In the weak disorder limit $\lambda \approx \alpha(\tau)W/\sqrt{3}$, where $\alpha(\tau)$ is a dimensionless parameter. At high driving frequencies $\alpha(\tau) = 1 + O(\tau^2)$. This approximation is valid if the period of driving is less than the radius of convergence of Eq. (3) [40]. At low frequencies, $\lim_{\tau \rightarrow \infty} \alpha(\tau) = \alpha_0$, where α_0 is a constant that depends on the model. In the strong disorder limit, assuming that the eigenvalues of $\delta V_F \tau$ are evenly distributed in the interval $[-\pi, \pi]$, we get $\lambda \tau \approx \pi/\sqrt{3}$. The value of λ plays the role of a phenomenological parameter in the model.

To this end, and before presenting the analytical machinery, we demonstrate our results in the context of

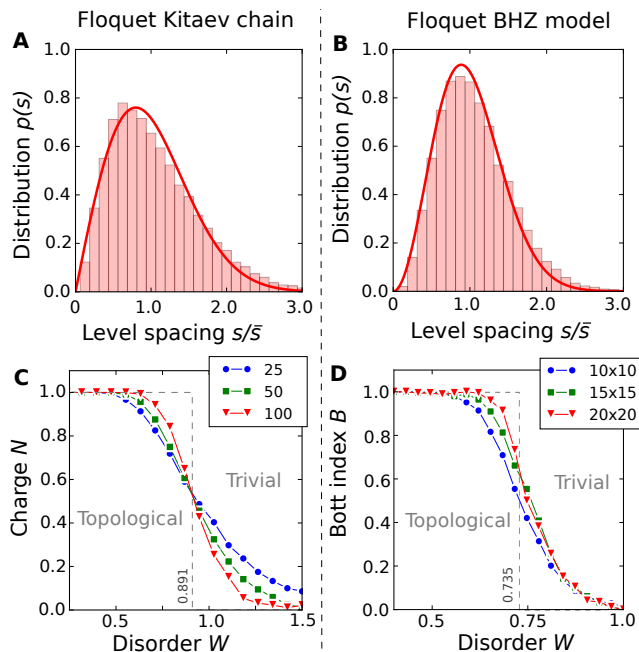


FIG. 2. **Effect of disorder.** **A, B** Level spacing distribution for the middle of the spectrum of δV_F for Floquet Kitaev chain and Floquet BHZ models, respectively, for $W = 0.5$. Red curves are the level spacing distribution for GOE (*A*) and GUE (*B*), respectively. **C, D** The topological charge and Bott index as a function of the disorder for the Kitaev chain and BHZ models, respectively. The dashed step function is the expected behavior in the thermodynamic limit. The parameters of the models are as in Fig. 3.

two widely studied models, the Kitaev chain and the 2D Bernevig-Hughes-Zhang (BHZ) model. For numerical simulations, both models can be represented as particular cases of a fermion hopping on a lattice:

$$H_0 = \sum_{\mathbf{r}, \mathbf{a} \in A} \left(\Gamma_{\mathbf{a}} |\mathbf{r}\rangle \langle \mathbf{r} + \mathbf{a}| + \text{h.c.} \right) + \mu \Gamma_0, \quad (5)$$

where $A = \{\mathbf{a}\}$ is the set of primitive vectors on the lattice, $\Gamma_{\mathbf{a}}$ and Γ_0 are Hermitian matrices, and μ is the chemical potential. We choose the driving field and disorder to be

$$V(t) = F\theta(t), \quad \delta V = \Gamma_0 \sum_{\mathbf{r}} h_{\mathbf{r}} |\mathbf{r}\rangle \langle \mathbf{r}|, \quad (6)$$

where $\theta(t) = \text{sgn}(\sin \Omega t)$, and $h_{\mathbf{r}}$ is uniformly random in $[-W, W]$.

As the first example, we take the Bogoliubovde Gennes Hamiltonian for the Kitaev chain [41], which has the form of Eq. (5) with $\Gamma_x = i\Delta\sigma_y + J\sigma_z$, $\Gamma_0 = \sigma_z$, and $F = f\sigma_z$. The σ_i s are the Pauli matrices, Δ is the superconducting pairing, $J > 0$ is the hopping constant, and f is the amplitude of the external driving. In the absence of driving, the clean system is an archetypal example of a

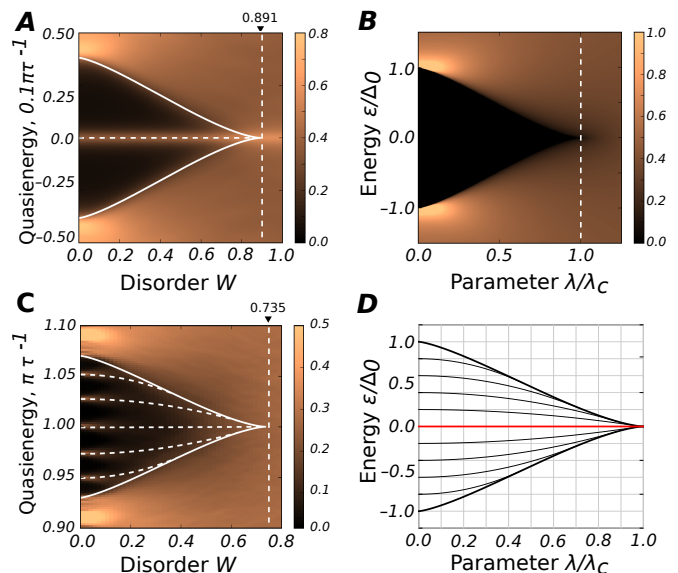


FIG. 3. **Density of states (DOS).** **A** DOS of Floquet 1D Kitaev chain of size $L = 10^2$ for $\Delta = 1$, $J = 1$, $\mu = 4.5$, $f = 1.5$ and $\tau = 2\pi/\Omega = 1.1$ (level width applied $\gamma = 10^{-2}\tau^{-1}$). White solid curve and dashed white line are the analytical gap prediction (Eq.(11)) with $\lambda = W$ and the Majorana state, respectively. **B** DOS of Floquet BHZ model on a square lattice 20×20 and mixed periodic (x -direction) and open (y -direction) boundary conditions near quasienergy $\varepsilon = \Omega/2$. (Level widening applied $\gamma = 0.2 \cdot 10^{-2}\tau^{-1}$). The white curve is the analytical gap prediction given by Eq.(11) with $\lambda = 0.9W$, and the dashed curves are the analytical prediction for behavior of the mid-gap states given by Eq.(12). **C** Analytic calculations of bulk DOS for the model Eq.(4), as described below Eq. (9). **D** Analytic result for the mid-gap states given by Eq.(12).

1D topological superconductor, exhibiting a topological phase transition at $|\mu| = 2J$. When $|\mu| < 2J$, the system is in the topological phase hosting two Majorana zero-energy modes at each end of the chain, and is in the trivial phase otherwise. However, recent proposals [16, 17] suggest that when $|\mu| > 2J$, the Kitaev chain may also exhibit topological states if a local periodic field is applied ($f \neq 0$). In this case, Majorana modes can exist for quasienergies $\varepsilon = 0$ and $\varepsilon = \Omega/2$. We focus on the stability of the $\varepsilon = 0$ Majorana mode against disorder present in the system, and we assume similar behavior for the $\varepsilon = \Omega/2$ mode.

Numerically, we find that strong disorder destroys the induced topological Floquet phase by closing the spectral gap. Fig. 2C demonstrates this transition for the average topological charge $N = -\langle \text{sign}(\text{Pf}(i\hat{H}_F)) \rangle_{\text{dis}}$, where \hat{H}_F is the Floquet Hamiltonian in the Majorana representation (it is Hermitian and purely imaginary), and Pf is Pfaffian. If $N = 1$, the system is in a topological phase, while in the disordered trivial phase $N = 0$. Vanishing of the gap corresponds to the transition from $N = 1$ to $N = 0$. Fig. 3A shows the closing of the gap at the crit-

ical disorder strength. The analytical predictions of the effective theory Eq.(4) with $\lambda = W$ are also presented in Fig. 3A. The analytical calculation of the gap (white solid curve) and zero-energy mode (white dashed line) show good agreements with exact diagonalization.

Similar results can be obtained in 2D by choosing a square lattice with $\Gamma_x = -i\frac{A}{2}\sigma_x + B\sigma_z$, $\Gamma_y = -i\frac{A}{2}\sigma_y + B\sigma_z$, and $M_{\mathbf{r}} = h_{\mathbf{r}} + (\Delta - 4B + f\text{sgn}(\sin \Omega t))\sigma_z$. Here A is a velocity parameter, B defines the inverse kinetic mass, Δ is the bulk band gap, and $h_{\mathbf{r}}$ is the static disorder. The long-wavelength limit of this model coincides with the seminal BHZ theory [42] $H_0 = \sum_{i=1}^3 d_i(\mathbf{k})\sigma_i$, where $d(\mathbf{k}) = (Ak_x, Ak_y, \Delta - B(k_x^2 + k_y^2))$. For $\Delta/B > 0$, the disordered system is characterized by the Bott index [43, 44] $C = 1$ and hosts topologically protected states at the edge. Similar to the Kitaev chain, the trivial phase $\Delta/B < 0$ can be converted into a topological phase by applying a periodic driving field $f \neq 0$. The effect of disorder is shown in Fig. 2D and Fig. 3C. In Fig. 3C, the white solid curve and dashed white curves are the gap and edge states, respectively; both are analytically computed. The discreteness of edge states is due to the finite size.

The efficacy of H_F^{eff} (Eq. (4)) in capturing the exact H'_F (Eq. (2)) is easily demonstrated in the models we studied by examining the matrix $\delta V_F = H_F - H_F|_{W=0}$. Remarkably, δV_F turns out to be a nonlocal matrix with level statistics close to the Wigner-Dyson law (Fig. 2A-B). Interestingly, the renormalized disorder δV_F approximately follows the GOE and GUE statistics for the 1D Kitaev chain and 2D BHZ Hamiltonian, respectively. Whether GOE or GUE level statistics is dictated by the dimension of the lattice is a question we leave for future work.

We proceed with our main goal of analytically solving spectral properties of H_F^{eff} (Eq. (4)). The main tool enabling this is free probability theory [45–48], which we now introduce (see the Supplemental Material and Ref. [48] for an applied overview). Free probability theory (FPT) extends the conventional probability theory to the noncommuting random variables setting. Recall the φ notation $\varphi(A) = (\mathbb{E}\text{Tr } A)/\dim(A)$, and $\overline{A^k} = A^k - \varphi(A^k)$. Two random matrices A and B are freely independent (or free) if all expectation values of cross-term correlators vanish in the infinite size limit. That is, $\varphi(\overline{A^{k_1} B^{l_1} \dots A^{k_n} B^{l_n}}) = 0$ (see Refs. [48, 49] for a comprehensive definition). The free independence is immediate if either A or B is chosen independently from the Gaussian ensemble. Therefore, in Eq. (4), H_F and λM are free.

The input to the theory is the Cauchy transform of the DOS of the summands $G_A(z) = \varphi((z - A)^{-1})$ and $G_B(z) = \varphi((z - B)^{-1})$. The integral representation of $\rho_A(\varepsilon)$, of matrix A is (similarly for B) is

$$G_A(z) = \frac{1}{2\pi i} \int_{\mathbb{R}} d\varepsilon \frac{\rho_A(\varepsilon)}{z - \varepsilon}. \quad (7)$$

The R transform is defined by $R_A(w) = G_A^{-1}(w) - w^{-1}$, where G_A^{-1} is the functional inverse (similarly for B). Recall that in standard probability theory, the additive quantity for sums of scalar random variables is the log characteristics. In FPT, the analogous additive quantity is the R transform, which in turn defines the Cauchy transform of the sum $G_{A+B}(\varepsilon)$. One then obtains the DOS from $G_{A+B}(\varepsilon)$, with the caveat that the technical challenge often is the inversion of $G_{A+B}(\varepsilon)$ to obtain the density. Below, H_F and λM replace A and B , respectively (see the Supplemental Material for technical details of what follows).

The R transform of H_F^{eff} in Eq.(4) is $R_{H_F^{\text{eff}}}(w) \equiv R_{H_F}(w) + R_{\lambda M}(w)$. This is equivalent to (see the Supplemental Material)

$$G_{H_{\text{eff}}}^{-1}(w) = G_{H_F}^{-1}(w) + G_{\lambda M}^{-1}(w) - \frac{1}{w}. \quad (8)$$

At energies not much larger than the Floquet band gap Δ_0 , the bulk DOS of the topological Hamiltonian H_F is approximated by $\rho_{H_F}(\varepsilon) \approx \rho_0\varepsilon/\sqrt{\varepsilon^2 - \Delta_0^2}$, where ρ_0 is the DOS in the vicinity of the gap. The DOS of λM is the well-known semicircle law $\rho_{\lambda M}(\varepsilon) = (2\pi\lambda^2)^{-1}\sqrt{4\lambda^2 - \varepsilon^2}$. The Cauchy transform $w \equiv G_{H_{\text{eff}}}(\varepsilon)$ can be derived from the condition Eq. (8), which is equivalent to

$$\varepsilon = \lambda^2 w + \frac{w^2 \Delta_0^2}{\sqrt{\pi^2 \rho_0^2 - w^2}}. \quad (9)$$

The DOS is then obtained from the imaginary part of the Cauchy transform, $\rho(\varepsilon) = \pi^{-1}\text{Im } w$. Energies ε for which w is real in Eq. (9) correspond to zero density of states – i.e., the band gap. The real solutions of w occur for $\lambda < \lambda_c$, with

$$\lambda_c = \sqrt{\Delta_0/\pi\rho_0}. \quad (10)$$

λ_c defines the critical point for the phase transition, where two bands merge and the gap vanishes (Fig. 3B). Let $\Delta(\lambda)$ be the band gap as a function of the effective disorder strength λ . For $|\varepsilon| < \Delta$, one has

$$\Delta(\lambda) = \Delta_0 \left[1 - (\pi\rho_0\lambda^2/\Delta_0)^{2/3} \right]^{3/2}, \quad \lambda < \lambda_c, \quad (11)$$

and $\Delta(\lambda) = 0$ for $\lambda \geq \lambda_c$.

We turn our attention to the behavior of the surface states energies ε_μ situated in the bulk band gap, where μ can be either a discrete or a continuous quantum number. To evaluate $\varepsilon_\mu(\lambda)$, one can use the fact that the number of surface states is small compared to bulk ones. This allows us to derive the spectrum, considering them as small corrections to the Cauchy transform (Eq.(7)).

In the Supplemental Material, we show that the resulting spectrum of midgap states satisfies $G_{H_F}(\varepsilon_\mu) = G_{H_{\text{eff}}}(\varepsilon_\mu(\lambda))$, which leads to

$$\varepsilon_\mu(\lambda) = \varepsilon_\mu \left(1 - \frac{\pi\rho_0\lambda^2}{\sqrt{\Delta_0^2 - \varepsilon_\mu^2}} \right), \quad \lambda < \lambda_c^\mu, \quad (12)$$

where λ_c^μ denotes the solution of $\varepsilon_\mu(\lambda_c^\mu) = \Delta(\lambda_c^\mu)$. The plots for $\varepsilon_\mu(\lambda)$ for different initial values ε_μ are shown in Fig. 3D. As seen there, the continuous spectrum of surface states never opens up a spectral gap.

Remark. – The theory is universal, in that the details of the underlying model, such as the dimension of the lattice, the period τ , or the DOS of the clean system, only enter through ρ_0 and Δ_0 .

To summarize, we demonstrated that the disorder effects on finite-frequency Floquet phases can be well approximated by generic random matrices (Eq. (4)). Using this and free probability theory, we analytically show that the topological phases in this regime are generically stable against disorder for a range of strength. The breakdown into the trivial phase typically happens at a critical disorder strength that is potentially many times larger than the spectral gap. The proposed theory allows us to compute the critical gap behavior and the corresponding critical exponents. The analytical prediction of the critical point can serve as a guide in experiments to search for topological phases in the presence of disorder more systematically and irrespective of the underlying model.

The utility of free probability theory for approximating spectral properties of physical systems extends beyond this Letter. On the one hand, it works in the more general settings in which perturbative analysis fails (e.g., in the current study, the regime of strong disorder and/or moderate frequency of driving). On the other hand, free convolution is an entirely new technique that can be added to the arsenal of the existing tools. We emphasize that the success of free probability theory does not rely on the disorder being generic (cf. Refs. [46, 47]).

Future research may include applying our techniques to time crystals [50] and other disordered systems, especially with many-body interactions for example, the treatment of the self-energy in self-consistent Born approximations [51]. We anticipate these methods to provide a new angle of attack on problems of disordered superconductivity and many-body localization.

We thank Iman Marvian. O. S. was supported by ExxonMobil-MIT Energy Initiative Fellowship. O. S. acknowledges MIT Externship program and partial support by IBM Research.

[1] H. Bernien, S. Schwartz, A. Keesling, H. Levine, A. Omran, H. Pichler, S. Choi, A. S. Zibrov, M. Endres, M. Greiner, *et al.*, *Nature* **551**, 579 (2017).
 [2] J. Zhang, G. Pagano, P. W. Hess, A. Kyprianidis, P. Becker, H. Kaplan, A. V. Gorshkov, Z.-X. Gong, and C. Monroe, *Nature* **551**, 601 (2017).
 [3] M. Bukov, L. D’Alessio, and A. Polkovnikov, *Adv. Phys.* **64**, 139 (2015).
 [4] A. Eckardt, *Rev. Mod. Phys.* **89**, 011004 (2017).

[5] T. Kitagawa, M. A. Broome, A. Fedrizzi, M. S. Rudner, E. Berg, I. Kassal, A. Aspuru-Guzik, E. Demler, and A. G. White, *Nat. Commun.* **3**, 882 EP (2012).
 [6] P. Hauke, O. Tieleman, A. Celi, C. Ölschläger, J. Simonet, J. Struck, M. Weinberg, P. Windpassinger, K. Sengstock, M. Lewenstein, and A. Eckardt, *Phys. Rev. Lett.* **109**, 145301 (2012).
 [7] M. Atala, M. Aidelsburger, J. T. Barreiro, D. Abanin, T. Kitagawa, E. Demler, and I. Bloch, *Nat. Phys.* **9**, 795 (2013).
 [8] Y. Wang, H. Steinberg, P. Jarillo-Herrero, and N. Gedik, *Science* **342**, 453 (2013).
 [9] E. J. Meier, F. A. An, and B. Gadway, *Nat. Commun.* **7**, 13986 (2016).
 [10] J. Cayssol, B. Dóra, F. Simon, and R. Moessner, *Phys. Status Solidi Rapid Res. Lett.* **7**, 101 (2013).
 [11] P. Titum, E. Berg, M. S. Rudner, G. Refael, and N. H. Lindner, *Phys. Rev. X* **6**, 021013 (2016).
 [12] F. Nathan, D. Abanin, E. Berg, N. H. Lindner, and M. S. Rudner, arXiv preprint arXiv:1712.02789 (2017).
 [13] L. J. Maczewsky, J. M. Zeuner, S. Nolte, and A. Szameit, *Nat. Commun.* **8**, 13756 (2017).
 [14] D. V. Else, B. Bauer, and C. Nayak, *Phys. Rev. Lett.* **117**, 090402 (2016).
 [15] S. Choi, J. Choi, R. Landig, G. Kucsko, H. Zhou, J. Isoya, F. Jelezko, S. Onoda, H. Sumiya, V. Khemani, C. von Keyserlingk, N. Y. Yao, E. Demler, and M. D. Lukin, *Nature* **543**, 221 (2017).
 [16] L. Jiang, T. Kitagawa, J. Alicea, A. R. Akhmerov, D. Pekker, G. Refael, J. I. Cirac, E. Demler, M. D. Lukin, and P. Zoller, *Phys. Rev. Lett.* **106**, 220402 (2011).
 [17] D. E. Liu, A. Levchenko, and H. U. Baranger, *Phys. Rev. Lett.* **111**, 047002 (2013).
 [18] A. Kundu and B. Seradjeh, *Phys. Rev. Lett.* **111**, 136402 (2013).
 [19] P. Bordia, H. Lüschen, U. Schneider, M. Knap, and I. Bloch, *Nat. Phys.* **13**, 460 (2017).
 [20] D. A. Abanin, E. Altman, I. Bloch, and M. Serbyn, arXiv preprint arXiv:1804.11065 (2018).
 [21] P. Ponte, A. Chandran, Z. Papić, and D. A. Abanin, *Ann. Phys.* **353**, 196 (2015).
 [22] C. W. von Keyserlingk and S. L. Sondhi, *Phys. Rev. B* **93**, 245145 (2016).
 [23] C.-Z. Chen, J. Song, H. Jiang, Q.-f. Sun, Z. Wang, and X. C. Xie, *Phys. Rev. Lett.* **115**, 246603 (2015).
 [24] D. V. Else and C. Nayak, *Phys. Rev. B* **93**, 201103 (2016).
 [25] Y. Bahri, R. Vosk, E. Altman, and A. Vishwanath, *Nat. Comm.* **6**, 7341 (2015).
 [26] P. Titum, N. H. Lindner, M. C. Rechtsman, and G. Refael, *Phys. Rev. Lett.* **114**, 056801 (2015).
 [27] P. Titum, N. H. Lindner, and G. Refael, *Phys. Rev. B* **96**, 054207 (2017).
 [28] V. Khemani, A. Lazarides, R. Moessner, and S. L. Sondhi, *Phys. Rev. Lett.* **116**, 250401 (2016).
 [29] Y. Gannot, arXiv preprint arXiv:1512.04190 (2015).
 [30] D. I. Pikulin, T. Hyart, S. Mi, J. Tworzydło, M. Wimmer, and C. W. J. Beenakker, *Phys. Rev. B* **89**, 161403 (2014).
 [31] J. Li, R.-L. Chu, J. K. Jain, and S.-Q. Shen, *Phys. Rev. Lett.* **102**, 136806 (2009).
 [32] C. W. Groth, M. Wimmer, A. R. Akhmerov, J. Tworzydło, and C. W. J. Beenakker, *Phys. Rev. Lett.* **103**, 196805 (2009).
 [33] C. W. von Keyserlingk, V. Khemani, and S. L. Sondhi,

- Phys. Rev. B **94**, 085112 (2016).
- [34] N. F. Mott, Phil. Mag. **22**, 7 (1970).
- [35] A. Klein, O. Lenoble, and P. Moller, Ann. Math. **166**, 549 (2007).
- [36] R. Ducatez and F. Huveneers, Ann. Henri Poincaré **18**, 2415 (2017).
- [37] K. Agarwal, S. Ganeshan, and R. N. Bhatt, Phys. Rev. B **96**, 014201 (2017).
- [38] T. Kuwahara, T. Mori, and K. Saito, Ann. Phys. **367**, 96 (2016).
- [39] M. L. Mehta, *Random matrices*, Vol. 142 (Elsevier, 2004).
- [40] Radius of convergence is given by $\int_0^{\tau} \|H(t)\| dt \leq \pi$, see Supplementary Material and [?].
- [41] A. Y. Kitaev, Phys. Usp. **44**, 131 (2001).
- [42] B. A. Bernevig, T. L. Hughes, and S.-C. Zhang, Science **314**, 1757 (2006).
- [43] T. A. Loring and M. B. Hastings, Europhys. Lett. **92**, 67004 (2011).
- [44] D. Toniolo, arXiv preprint arXiv:1708.05912 (2017).
- [45] R. S. James A. Mingo, *Free Probability and Random Matrices* (Springer New York, 2017).
- [46] R. Movassagh and A. Edelman, Phys. Rev. Lett. **107**, 097205 (2011).
- [47] J. Chen, E. Hontz, J. Moix, M. Welborn, T. Van Voorhis, A. Suárez, R. Movassagh, and A. Edelman, Phys. Rev. Lett. **109**, 036403 (2012).
- [48] R. Movassagh and A. Edelman, arXiv preprint arXiv:1710.09400 (2017).
- [49] A. Nica and R. Speicher, *Lectures on the combinatorics of free probability*, Vol. 13 (Cambridge University Press, 2006).
- [50] W. Berdanier, M. Kolodrubetz, S. Parameswaran, and R. Vasseur, arXiv preprint arXiv:1803.00019 (2018).
- [51] A. A. Abrikosov and L. P. Gor'kov, Zhur. Eksptl'. i Teoret. Fiz. **39** (1960).

Supplemental Material

CALCULATION OF SPECTRUM USING FREE PROBABILITY THEORY

Free probability theory (FPT) extends the conventional probability theory to the setting in which the random variables do not commute [1, 2]. The canonical examples of such random variables are random matrices. Since its discovery in 1980's, FPT has been mainly a sub-field of pure mathematics. However, in recent times, it has been distilled for applications and shown to have potentials for a wide set of problems of applied interest (see [3] for details and an overview of *applied* FPT).

Suppose we are interested in the density of states (eigenvalue distribution) of the sum

$$A = A_1 + A_2, \quad (\text{S.1})$$

where the densities of A_1 and A_2 are known. If matrices are freely independent (see [1] for exact definition), FPT provides the distribution $\rho(\varepsilon)$ of matrix A from the densities $\rho_1(\varepsilon)$ and $\rho_2(\varepsilon)$ of matrices A_1 and A_2 . The input to the theory is the *Cauchy transform* of the densities of the summands. The Cauchy transform of $\rho_\alpha(\varepsilon)$ is defined by

$$G_\alpha(z) = \frac{1}{2\pi i} \int_{-\infty}^{\infty} d\varepsilon \frac{\rho_\alpha(\varepsilon)}{z - \varepsilon}. \quad (\text{S.2})$$

It is good practice to introduce a new variable, w , to denote the Cauchy transform $w \equiv G(z)$.

Analogous to log-characteristics in conventional probability theory, the key additive quantity in FPT is the R-transforms:

$$R = R_1 + R_2, \quad R_\alpha(w) \equiv G_\alpha^{-1}(w) - \frac{1}{w}, \quad \alpha = 1, 2 \quad (\text{S.3})$$

where $z = G_\alpha^{-1}(w)$ is the functional inverse.

Technically, computation of the density of states of matrix A can be performed in four steps:

1. Input to the theory are the Cauchy transforms of the summands denoted by $G_1(z)$ and $G_2(z)$, which one obtains using Eq.(S.2),
2. Computation of the functional inverse for Greens functions $G_1^{-1}(w)$ and $G_2^{-1}(w)$;
3. One then finds the inverse Cauchy transform for sum of matrices $w = G^{-1}(w)$ using formula Eq.(S.3) ;
4. Then one obtains the Cauchy transform of the sum, $w = G(z)$, by inversion. Lastly the density is computed by

$$\rho(\varepsilon) = \frac{1}{\pi} \lim_{\eta^+} \{\text{Im}(G(z))\}, \quad (\text{S.4})$$

where $\frac{1}{\pi} \lim_{\eta^+} [\text{Im}(G(z))]$ means taking a limit from above to the branch cut of $G(z)$.

Steps 2 and 4 require computing the functional inverse of corresponding Greens functions. In the generic case, it would require a numerical computation. However, in some physically relevant cases, the inversion can be performed analytically, as it is shown below.

Problem of Random Disorder Correction

Here we apply this method to the sum of matrices Eq.(3) in the main text describing the effect of disorder on the clean system Hamiltonian H_F :

$$H_F^{\text{eff}} = H_F + \lambda M \quad (\text{S.5})$$

where λ is the real parameter that quantifies the strength of disorder.

Let us consider a Floquet Hamiltonian H_F describing a d -dimensional non-interacting topological system of linear size L with $N = N_B + N_S$ system eigenstates, where $N_B \sim L^d$ is number of bulk states and $N_S \sim L^{d-1}$ is number of surface states. The density of states of the clean system is simply the sum of the bulk and surface states densities

$$\rho(\varepsilon) = \rho_B(\varepsilon) + \rho_S(\varepsilon) \quad (\text{S.6})$$

We assume that the band gap Δ_0 in the system is negligible compared to the bandwidth Γ , $\Delta_0 \ll \Gamma$. This allows one to neglect the energy dependence of the DOS outside the gap in systems with quadratic spectrum, including superconductors. In this case, the DOS near the gap has the universal and dimension-independent form:

$$\rho_B(\varepsilon) \approx \frac{\rho_0 |\varepsilon|}{\sqrt{\varepsilon^2 - \Delta_0^2}}, \quad \Delta_0 \leq |\varepsilon| \ll \Gamma \quad (\text{S.7})$$

where ρ_0 and Δ_0 depend on the details of the model.

We only consider the surface states which are inside the gap. Let ε_μ represent the spectrum of surface states (discrete for $d = 1$ or continuous for $d \geq 2$), then the corresponding surface states contribution to DOS is

$$\rho_S(\varepsilon) = \frac{\alpha}{N_S} \sum_{\mu} \delta(\varepsilon - \varepsilon_{\mu}), \quad |\varepsilon| < \Delta_0 \quad (\text{S.8})$$

where $\alpha = N_S/N \sim 1/L$ is a small parameter. Both approximated bulk density expression Eq.(S.7) and surface density expression Eq.(S.8) are dimension-independent and universal across many models.

The disorder contribution is modeled by a Hermitian generic random matrix whose distribution is the well-known semicircle law

$$\rho_{\lambda M}(\varepsilon) = \frac{1}{2\pi\lambda^2} \sqrt{4\lambda^2 - \varepsilon^2}. \quad (\text{S.9})$$

Comment: The underlying gaussian ensemble may be GOE or GUE.

Density of Bulk States

Since α in Eq.(S.8) vanishes in the thermodynamic limit, one may ignore the influence of surface states on the bulk spectrum to estimate the behavior of the bulk states. The Cauchy transform is

$$G_{H_F}(z) = \frac{1}{N} \lim_{\eta \rightarrow 0} \text{Tr} \frac{1}{z - H_F - i\eta} = \lim_{\eta \rightarrow 0} \int_{-\infty}^{\infty} d\varepsilon \frac{\rho_B(\varepsilon)}{z - (\varepsilon + i\eta)} + O(\alpha) = \frac{z}{\sqrt{\Delta_0^2 - z^2}} + O(\alpha) \quad (\text{S.10})$$

where, to simplify the expressions, we drop $\pi\rho_0$ by rescaling $\lambda \rightarrow \pi\rho_0\lambda$, $z \rightarrow \pi\rho_0z$, and $\Delta_0 \rightarrow \pi\rho_0\Delta_0$.

The Cauchy transform of random matrix spectral density is

$$G_{\lambda M}(z) = \lim_{\eta \rightarrow 0} \int_{-\infty}^{\infty} d\varepsilon \frac{\rho_{\lambda M}(\varepsilon)}{z - (\varepsilon + i\eta)} = \frac{1}{2\lambda^2} (z - \sqrt{z^2 - 4\lambda^2}) \quad (\text{S.11})$$

The R-Transform of the two distributions ρ_B and $\rho_{\lambda M}$ are, respectively, given by

$$R_{H_F}(w) = G_{H_F}^{-1}(w) - \frac{1}{w} = \frac{\Delta_0 w}{\sqrt{1 + w^2}} - \frac{1}{w} \quad (\text{S.12})$$

$$R_{\lambda M}(w) = G_{\lambda M}^{-1}(w) - \frac{1}{w} = \lambda^2 w \quad (\text{S.13})$$

We now use the key additivity property of the R-transform, to obtain

$$R_{H_F^{\text{eff}}}(w) = R_{H_F}(w) + R_{\lambda M}(w) = \lambda^2 w + \frac{\Delta_0 w}{\sqrt{1 + w^2}} - \frac{1}{w} \quad (\text{S.14})$$

With the R-transform of the sum in hand, we need to reverse obtain the actual density of the sum under the freeness assumption. The inverse Cauchy transform of the sum is $z \equiv G_{H_F^{\text{eff}}}^{-1}(w)$

$$G_{H_F^{\text{eff}}}^{-1}(w) = R_{H_F^{\text{eff}}}(w) + \frac{1}{w} = w \left(\lambda^2 + \frac{\Delta_0}{\sqrt{1 + w^2}} \right) \quad (\text{S.15})$$

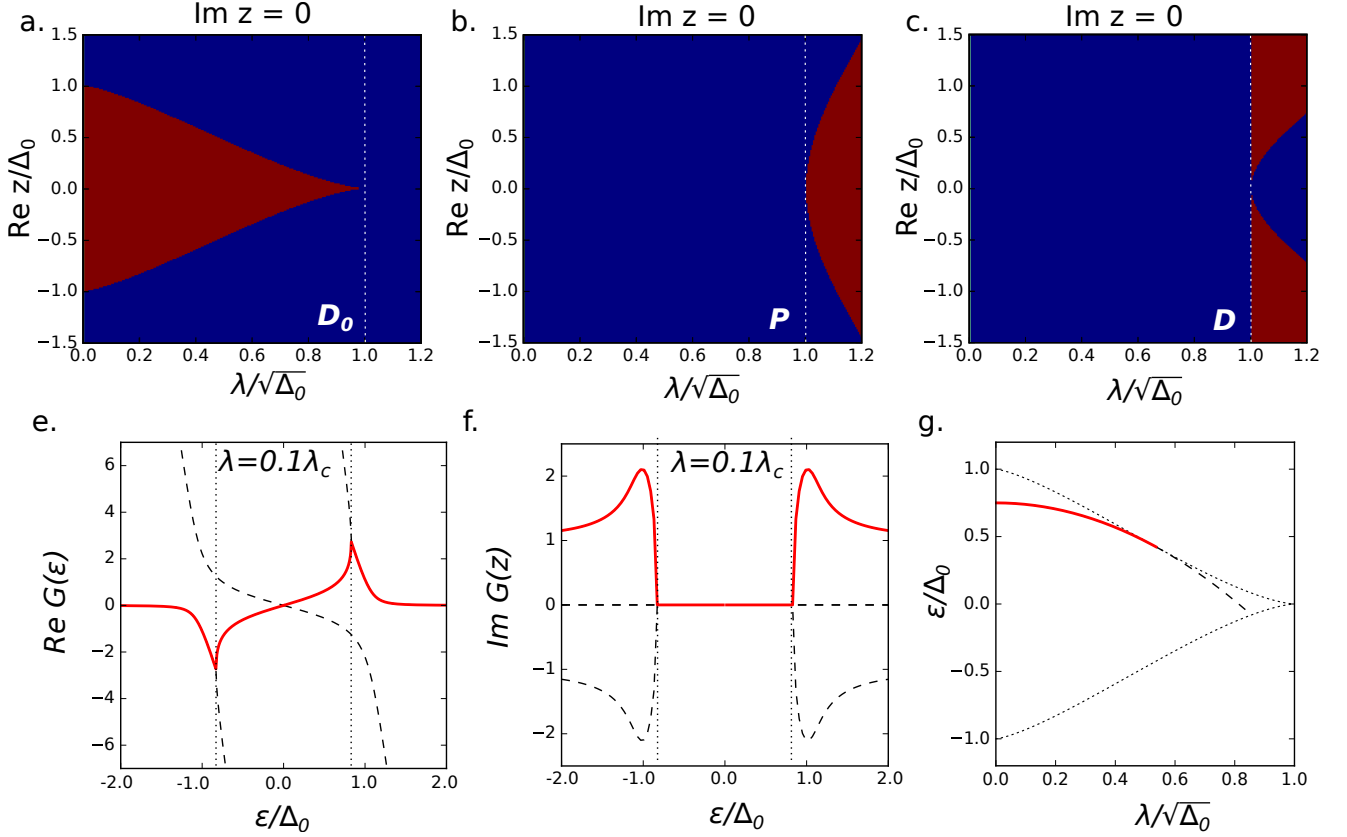


FIG. S1. **Details of analytical solution.** a.-c. Sign of discriminant $D_0(z, \Delta_0, \lambda)$ Eq.(S.18) and polynomials $P(z, \Delta_0, \lambda)$ and $D(z, \Delta_0, \lambda)$ Eq.(S.19) as function of z/Δ_0 taken at real z , and parameter $\lambda/\sqrt{\Delta_0}$. Region of positive parameter are red, regions with negative parameters are blue. The region where roots are purely real (region of spectral gap) coincides with the region of positive discriminant $D_0 > 0$. e.-f. Real and imaginary part of the solution for real z . Red lines represent the physically relevant solution of Eq.(S.16). Black dashed lines represent other possible solutions. Black dotted lines show edges of the gap g. Midgap state solution. Red line denotes the physical solution for midgap state. Black dashed line represent the midgap solution due to non-physical solution for G_H .

This equation needs to be inverted, and the inversion leads to solving the following polynomial equation

$$aw^4 + bw^3 + cw^2 + dw + e = 0, \quad (\text{S.16})$$

where the coefficients are defined as

$$a = \lambda^4, \quad b = -2z\lambda^2, \quad c = \lambda^4 + z^2 - \Delta_0^2, \quad d = -2z\lambda^2, \quad e = z^2. \quad (\text{S.17})$$

Let us consider only real values of z . The discriminant of the polynomial is of the form

$$\begin{aligned} D_0(\varepsilon, \Delta_0, \lambda) &= 256a^3e^3 - 192a^2bde^2 - 128a^2c^2e^2 + 144a^2cd^2e - 27a^2d^4 + 144ab^2ce^2 - 6ab^2d^2e \\ &\quad - 80abc^2de + 18abcd^3 + 16ac^4e - 4ac^3d^2 - 27b^4e^2 + 18b^3cde - 4b^3d^3 - 4b^2c^3e + b^2c^2d^2 \\ &= -16\Delta_0^2\lambda^4z^2 \left(z^6 + 3(\lambda^4 - \Delta_0^2)z^4 + 3(\Delta^4 + 7\Delta_0^2\lambda^4 + \lambda^8)z^2 + (\lambda^4 - \Delta_0^2)^3 \right). \end{aligned} \quad (\text{S.18})$$

Two other quantities characterizing the quartic equation are

$$P(\varepsilon, \Delta_0, \lambda) = 8ac - 3b^2 = -4\lambda^4 (2\Delta_0^2 + z^2 - 2\lambda^4) \quad (\text{S.19})$$

$$D(\varepsilon, \Delta_0, \lambda) = 64a^3e - 16a^2bd - 16a^2c^2 + 16ab^2c - 3b^4 = -16\lambda^8 (\Delta_0^2 - \lambda^4) (\Delta_0^2 - \lambda^4 + 2z^2) \quad (\text{S.20})$$

Remark : To have a gap, one seeks the set of parameters for which there is *no support* for DOS $\rho(\varepsilon)$. Recall that

$$\rho(\varepsilon) = \pi^{-1} \lim_{\eta^+} \{\text{Im}(G_{H_F^{\text{eff}}}(z))\}; \quad (\text{S.21})$$

therefore we seek four real solutions to the quartic equation. This corresponds to having $P < 0$, and $D < 0$.

As can be seen from the analysis of the signs of D_0 , P , and D , the solution of Eq.(S.16) has zero imaginary part only in the region where $D_0 > 0$ (see Fig. S1). Therefore, the gap will be defined by the solution of $D_0(\varepsilon, \Delta_0, \lambda) = 0$ (excluding solution $z = 0$). In the explicit form it is equal to:

$$z^6 + 3(\lambda^4 - \Delta_0^2)z^4 + 3(\Delta_0^4 + 7\Delta_0^2\lambda^4 + \lambda^8)z^2 + (\lambda^4 - \Delta_0^2)^3 = 0. \quad (\text{S.22})$$

Two real solutions of this equation $z = \pm z_0$ define the edges of spectral gap $\Delta(\lambda) = z_0$. It can be written in a compact form (here we restore the $\pi\rho_0$ factor we dropped starting at Eq.(S.10))

$$\Delta(\lambda) = \left(\Delta_0^{2/3} - (\pi\rho_0\lambda^2)^{2/3} \right)^{3/2}. \quad (\text{S.23})$$

As expected, at zero disorder $\Delta(0) = \Delta_0$ and decreases with disorder strength. At the critical strength $\lambda_c = \sqrt{\Delta_0/\pi\rho_0}$, the gap closes and the system transitions into the metallic phase. Using Taylor expansion, we obtain the behavior of the gap in the vicinity of the critical point:

$$\Delta(\lambda) = \Delta_0 \frac{8}{3\sqrt{3}} \frac{|\lambda - \lambda_c|^{3/2}}{\lambda_c^{3/2}} + O(|\lambda - \lambda_c|^{5/2}), \quad \lambda < \lambda_c \quad (\text{S.24})$$

From this one immediately reads off the critical exponents for such type of transition

$$\nu z = 3/2 \quad (\text{S.25})$$

Since we neither specify exactly the Hamiltonian of the system nor its dimensionality, the condition Eq. (S.25) is rather widely applicable to a variety of systems.

Remark : Eq. (S.16) is quartic and can be analytically solved. Nevertheless, obtaining the imaginary part of the solution, and consequently, DOS yields unwieldy expressions. Therefore, we obtain the solutions of Eq.(S.16) numerically using NumPy Python package. The results are presented in Fig.3C of the main text.

Density of Surface States

The surface states give a contribution to the total DOS suppressed by a factor of L^{-1} . This enables one to calculate the corresponding DOS using perturbation theory. The Cauchy transform for the Floquet Hamiltonian H_F , including the surface states, reads as

$$\tilde{G}_{H_F}(z) = G_{H_F}(z) + \alpha \frac{2\pi}{N_S} \lim_{\eta \rightarrow 0} \sum_{\mu=1}^{N_S} \frac{1}{z - \varepsilon_\mu^s - i\eta} \quad (\text{S.26})$$

We use the power expansion ansatz for the inverse of the Cauchy transform to be

$$\tilde{G}_{H_F}^{-1}(w) = G_{H_F}^{-1}(w) + \alpha A(w) + O(\alpha^2) \quad (\text{S.27})$$

where $A(w)$ is a surface correction which can be obtained from the consistency condition

$$\tilde{G}_{H_F}(\tilde{G}_{H_F}^{-1}(w)) = w \quad (\text{S.28})$$

Inserting Eq.(S.26) and Eq. (S.27) into Eq.(S.28), one derives

$$A(w) = -\frac{1}{N} \frac{2\pi}{N_S} \sum_{\mu} \frac{1}{G_{H_F}^{-1}(w) - \varepsilon_\mu - i\eta}, \quad \mathcal{N} = \left. \frac{\partial G_{H_F}(z)}{\partial z} \right|_{z=G_{H_F}^{-1}(w)} = \frac{1}{\Delta_0} (1+w^2)^{3/2} \quad (\text{S.29})$$

Using Eq.(S.15) we calculate the Cauchy transform of the effective Hamiltonian to get

$$\tilde{G}_{H_F^{\text{eff}}}^{-1}(w) = G_{H_F^{\text{eff}}}^{-1}(w) + \alpha A(w) + O(\alpha^2). \quad (\text{S.30})$$

Taking the functional inverse we use a power series expansion once more to get

$$\tilde{G}_H(z) = G_H(z) + \alpha B(z) + O(\alpha^2), \quad (\text{S.31})$$

where

$$B(z) = -\frac{1}{\mathcal{N}_2} A\left(G_{H_F^{\text{eff}}}(z)\right), \quad \mathcal{N}_2 = \left. \frac{\partial G_{H_F^{\text{eff}}}^{-1}(w)}{\partial w} \right|_{w=G_{H_F^{\text{eff}}}(z)} = \lambda^2 + \frac{\Delta_0}{(1+w^2)^{3/2}} \quad (\text{S.32})$$

$$B(z) = g \frac{2\pi}{N'_S} \sum_{\mu=1}^{N_S} \frac{1}{G_{H_F}^{-1}(G_H(z)) - \varepsilon_\mu - i0_+}, \quad g = \frac{N_S}{1 + \lambda^2 \Delta_0^{-1} (1 + G_{H_F^{\text{eff}}}(z)^2)^{3/2}}. \quad (\text{S.33})$$

For real z , if the condition $|z| < \Delta(\lambda)$ is satisfied, the prefactor g is real, and the midgap states' energies ε'_μ are defined by the new poles:

$$\varepsilon_\mu = G_{H_F}^{-1}(G_{H_F^{\text{eff}}}(\varepsilon'_\mu)). \quad (\text{S.34})$$

This condition leads to the following solution

$$\varepsilon'_\mu = \varepsilon_\mu \left(1 - \frac{\pi \rho_0 \lambda^2}{\sqrt{\Delta_0^2 - \varepsilon_\mu^2}} \right), \quad \lambda < \lambda_c^u \quad (\text{S.35})$$

This expression describes continuous deformation of the surface states spectrum without opening the gap.

DISORDER EFFECT ON FLOQUET TOPOLOGICAL SYSTEMS

As discussed in the main text, disorder added to a Floquet topological can destroy the topological phase.

To support the general analytical framework above, we now apply it to specific example to demonstrate the signatures of disorder-induced phase transition in finite size Floquet systems. We consider two non-interacting Floquet topological models: Kitaev chain [4] and Bernevig-Hughes-Zhang model [5]. In both cases, we study a time-periodic Hamiltonian in the form

$$H(t) = H_0 + V\theta(t), \quad \theta(t) = \begin{cases} +1, & n\tau < t \leq n\tau + \tau/2, \\ -1, & n\tau + \tau/2 < t \leq (n+1)\tau, \end{cases} \quad (\text{S.36})$$

where H_0 describes disordered insulator with trivial band topology, V is a local driving field, and τ is driving period. We perform our analysis by studying Floquet Hamiltonian, which is a functional of H_0 and V

$$H_F = H_F\{H_0, V\} = \frac{i}{\tau} \log \left(e^{-i(H_0-V)\tau/2} e^{-i(H_0+V)\tau/2} \right) \quad (\text{S.37})$$

We study the behavior of the gap in quasi-energy spectrum of H_F and its topological invariants as a function of static disorder. Also, to justify our approximations, we study the structure of disorder corrections to the Floquet Hamiltonian.

1D Example: Kitaev chain

Kitaev chain is an example of 1D topological superconductor [4]. In terms of electron operators in Fock space, the Kitaev chain Hamiltonian and corresponding driving field can be written as

$$\hat{H}_0 = (Jc_i^\dagger c_{i+1} + \text{h.c.}) + (\mu + h_i)c_i^\dagger c_i - (Dc_i c_{i+1} + \text{h.c.}), \quad \hat{V} = fc_i^\dagger c_i \quad (\text{S.38})$$

where c_i is an electron creation operator at site i , $J > 0$ is hopping constant, $D > 0$ is the superconducting gap, $\mu > 0$ is chemical potential, and $h_i \in [-W, W]$ is on-site random disorder. For numerical study, it is convenient to consider the Bogoliubov-de Gennes (BdG) form of the Hamiltonian H_0 and driving field V defined such that

$$\hat{H}_0 = \hat{C}^\dagger H_0 \hat{C}, \quad \hat{V} = \hat{C}^\dagger V \hat{C}, \quad (\text{S.39})$$

where $\hat{C} = \{c_1 \dots c_L, c_1^\dagger \dots c_L^\dagger\}$, and L is size of the system.

As a result, the exact form of BdG Hamiltonian can be written as $2L \times 2L$ matrices

$$H_0 = \sum_i \left((J\sigma_z + iD\sigma_y)|i\rangle\langle i+1| + \text{h.c.} \right) + (\mu + h_i)\sigma_z|i\rangle\langle i|, \quad V = \sum_i f\sigma_z|i\rangle\langle i| \quad (\text{S.40})$$

where σ_i are 2×2 Pauli matrices. This expression can be compared to Eqs.(5)-(6) in the main text.

For a particular choice of parameters corresponding to trivial static phase (we use $J = D = 1$, $\mu = 4.5$, and $f = 1.5$), the drive system exhibits several transitions at finite driving frequency with 0-quasienergy or/and π -quasienergy Majorana states. We focus on stability of 0-quasienergy Majorana state at driving period $\tau = 1.1$ characterized by quasienergy gap $\Delta_0 \approx 0.12 \tau^{-1} \ll \Omega$ and density of states $\rho_0 \approx 0.32 \tau$. The density of states of resulting Floquet Hamiltonian H_F Eq.(S.37) for the system size $L = 10^2$ is shown in Fig. 3A in the main text (on the right).

The topological invariance for Floquet Hamiltonian can be computed similar to the equilibrium Majorana fermion [6] by:

$$Q = Q_0 Q_\pi = \text{sign} \left(\text{Pf}(iH_F^m) \right), \quad H_F^m = U_m H_F U_m^\dagger \quad (\text{S.41})$$

where Q_0 , Q_π is topological charges for zero-quasienergy and π Majorana states correspondingly, H_F is Floquet Hamiltonian for the time dependent Hamiltonian with periodic boundary conditions, U_m is a unitary transformation to the basis of Majorana fermions converting H_F into skew-symmetric matrix H_F^m , $I_c = \sum_i |i\rangle\langle i|$ is the identity operator in coordinate basis, and $\text{Pf}(\cdot)$ is a Pfaffian.

We suppose that disorder does not destroy π -quasienergy Majorana fermion which has much larger gap. Then, disorder induced transition for 0-quasienergy Majorana state can be characterized by the parameter

$$N = -\langle Q \rangle_{\text{dis}} \quad (\text{S.42})$$

If gapped topological phase $Q = -1$, thus $N = 1$. In disordered gapless trivial phase the charge $Q = \pm 1$ with equal probability depending on disorder realization, i.e. $N = \langle Q \rangle_{\text{dis}} = 0$. The transition for the parameters chosen above is shown on Fig 2c in the main text.

Let us estimate the radius of convergence of the series for Floquet Hamiltonian in the case $\Delta = J$. For this, we use the criterion of convergence of Magnus expansion $\int_0^\tau \|H(t)\| dt \leq \pi$ [7]. Let us first focus on the system without disorder. The spectrum of the Kitaev chain is

$$\varepsilon_k^i = \pm \sqrt{(\mu_i + J \cos k)^2 + J^2 \sin^2 k} \quad (\text{S.43})$$

where $k \in [-\pi, \pi]$ is the wavenumber, $i = 1$ correspond to the instantaneous Hamiltonian during the first half of the step driving $n\tau < t < (n + \frac{1}{2})\tau$, and $i = 2$ is for the second part $(n + \frac{1}{2})\tau < t < (n + 1)\tau$, and n is an integer.

Then we can derive that for any sign of μ_i the following holds

$$\int_0^\tau \|H(t)\| dt = \frac{\tau}{2} \left(\max_k |\varepsilon_k^1| + \max_k |\varepsilon_k^2| \right) = \tau(J + \bar{\mu}), \quad \bar{\mu} = \frac{1}{2}(|\mu_1| + |\mu_2|). \quad (\text{S.44})$$

Therefore the convergence of Magnus expansion is guaranteed for $\tau < \tau_c$, where $\tau_c = \pi/(J + \bar{\mu})$. Adding disorder typically increases the bandwidth of the system. This result in a radius of convergence that is upper-bounded by that of the clean system. For the system shown in Fig. 3A in the main text, $J = \Delta = 1.0$, $f = 1.5$, $\mu_1 = \mu - f = 3.0$ and $\mu_2 = \mu + f = 6.0$, which gives the radius of convergence $\tau_c \approx 0.57$.

2D example: Bernevig-Hughes-Zhang model

The Bernevig-Hughes-Zhang (BHZ) model is paradigmatic example of 2D topological insulator [5]. In this work we consider a discretized version of BHZ model on a square lattice of size $L_x \times L_y$ written as

$$H_0 = \sum_{x,y} \left[\left(\Gamma_x |x,y\rangle\langle x+1,y| + \Gamma_y |x,y\rangle\langle x,y+1| + \text{h.c.} \right) + M_{x,y} |x,y\rangle\langle x,y| \right], \quad V(t) = \sum_{x,y} f\sigma_z |x,y\rangle\langle x,y| \quad (\text{S.45})$$

where x and y are integers corresponding to the coordinates of the site on the square lattice. We choose Γ_x, Γ_y and $M_{x,y}$ to be 2×2 matrices

$$\Gamma_x = -i\frac{A}{2}\sigma_x + B\sigma_z, \quad \Gamma_y = -i\frac{A}{2}\sigma_y + B\sigma_z, \quad M_{x,y} = h_{x,y} + (\mu - 4B)\sigma_z \quad (\text{S.46})$$

where $h_{x,y} \in [-W, W]$ is on-site scalar disorder.

In the long wavelength limit the discrete Hamiltonian Eq.(S.45) reduces to the conventional form of BHZ Hamiltonian:

$$H_0 = A\hat{p}_x\sigma_x + A\hat{p}_y\sigma_y + (\mu - B(\hat{p}_x^2 + \hat{p}_y^2))\sigma_z + h(x, y), \quad V = f\sigma_z \quad (\text{S.47})$$

where $\hat{p}_x = -i\partial_x$ and $\hat{p}_y = -i\partial_y$ are continuous momentum operators, and $h(x, y)$ is static disorder in continuous limit.

Similar to the Kitaev chain, at certain parameters describing non-topological case (we use $A = 0.25, B = -0.25, \mu = 1$) and resonant driving (we use $f = 1$ and $\Omega = 2\pi/T = 0.4$), the driven system exhibits a topological phase around π quasienergy. DOS of the resulting Floquet Hamiltonian H_F for system size $L_x = 20$ (periodic b.c.), $L_y = 20$ (open b.c.) is shown in Fig. 2B in the main text (the color plot). The transition for the parameters chosen above is shown on Fig. (2)D in the main text.

To define the topological invariant, we use Bott index (BI) as topological invariant in the system. BI is used in number of previous works [8, 9] and is known to be equivalent to Chern number in presence of translational symmetry [10, 11]. Let us consider a two-band insulator. To define BI, first let us define a pair of unitary operators U_1 and U_2 represented by $L_x L_y \times L_x L_y$ matrices such that:

$$\mathcal{P}_E e^{2\pi i X} \mathcal{P}_E = W \begin{pmatrix} 0 & 0 \\ 0 & U_1 \end{pmatrix} W^\dagger, \quad \mathcal{P}_E e^{2\pi i Y} \mathcal{P}_E = W \begin{pmatrix} 0 & 0 \\ 0 & U_2 \end{pmatrix} W^\dagger \quad (\text{S.48})$$

where \mathcal{P}_E is a projector on the lower band, operators $X = L_x^{-1} \sum_{x,y} x|x, y\rangle\langle x, y|$ and $Y = L_y^{-1} \sum_{x,y} y|x, y\rangle\langle x, y|$. The unitary transformation W is chosen such that

$$\mathcal{P}_E = W \begin{pmatrix} 0 & 0 \\ 0 & I \end{pmatrix} W^\dagger \quad (\text{S.49})$$

BI is defined as

$$B = \frac{1}{2\pi} \text{ImTr} \log(U_1 U_2 U_1^\dagger U_2^\dagger) \quad (\text{S.50})$$

The values of B for each disorder realizations are integer even for finite system size. At the same time, disorder-averaged values for finite system can be an arbitrary real number.

Properties of Renormalized Disorder

The driving-renormalized disorder δV_F is defined as corrections to the Floquet Hamiltonian,

$$\delta V_F = i \log U'_F - i \log U_F \quad (\text{S.51})$$

where δV is the original local disorder. A formal expansion can be used to represent δV_F by

$$\delta V_F \equiv \sum_{\ell \geq 1} \delta V_\ell \tau^{\ell-1}, \quad (\text{S.52})$$

where the terms in the expansion are

$$\delta V_1 = \delta V, \quad \delta V_\ell = \frac{1}{\tau^\ell} \left[K_\ell \{ H(t) + \delta V \} - K_\ell \{ H(t) \} \right], \quad (\text{S.53})$$

and K_ℓ are the Magnus expansion coefficients. First three coefficients are

$$K_1 \{ A(t) \} = \int_0^\tau dt A(t), \quad K_2 \{ A(t) \} = \frac{1}{2} \int_0^\tau dt_1 \int_0^{t_1} dt_2 [A(t_1), A(t_2)], \quad (\text{S.54})$$

$$K_3 \{ A(t) \} = \frac{1}{6} \int_0^\tau dt_1 \int_0^{t_1} dt_2 \int_0^{t_2} dt_3 \left([A(t_1), [A(t_2), A(t_3)]] + [A(t_3), [A(t_2), A(t_1)]] \right). \quad (\text{S.55})$$

At large driving frequency, renormalization is weak and δV_F is close to the original disorder δV .

To demonstrate this we visualize the statistics of level spacings of the spectrum of δV_F defined by $\text{Spec}(\delta V_F) \equiv \{v_n\}$, where $v_1 \leq v_2 \leq \dots \leq v_{max}$. The consecutive level spacings are defined by

$$s_n \equiv v_{n+1} - v_n. \quad (\text{S.56})$$

We focus on level spacings in ε -vicinity of the center of the spectrum, namely $\bar{v} - \varepsilon S < s_n < \bar{v} + \varepsilon S$, where $S = v_{max} - v_1$.

We compare the distribution of s_n to GOE and GUE defined by

$$\text{GOE} : \quad p_1(s) = \frac{\pi}{2} s \exp\left(-\frac{\pi}{4} s^2\right), \quad \text{GUE} : \quad p_2(s) = \frac{32}{\pi^2} s^2 \exp\left(-\frac{4}{\pi} s^2\right) \quad (\text{S.57})$$

The level statistics of the renormalized disorder operator δV_F in the vicinity of $\varepsilon = 0.1$ to the center is shown on Fig. 2A. Notably, the spacing of the disorder corrections for Kitaev chain is closer to GOE, while BHZ disorder correction is better described by GUE.

As expected, the effect of δV_F in spectral properties of the Floquet is similar to GRM. Hence, it may not lead to Anderson localization in low dimensions.

We, however, do not believe that δV_F can always be replaced by GRM. For example, δV_F must respect causality and Lieb-Robinson bounds characterized by velocity $v_{LR} \sim T$. This property cannot be captured by a GRM. Although, we believe that spectral properties of matrix $H_F + \delta V_F$ can be accurately described if we replace δV_F by GRM. As can be seen the numerical results give good agreements to the analytical formulas.

Lastly, we derive equations that quantify the dependence of the *effective* disorder strength λ on the period τ and the disorder strength W . Let us consider the particular form of driving in Eq. (S.36) and apply Eq. (S.53) to derive the Floquet disorder correction. To the lowest orders we have

$$\delta V_F = \delta V - \frac{\tau}{4} [\delta V, V] + \frac{\tau^2}{24} [\delta V, [V, H_0]] + O(\min(W^2 \tau^3, W \tau^4)) \quad (\text{S.58})$$

Assuming that $\delta V = \sum_{\mathbf{r}} h_{\mathbf{r}} |\mathbf{r}\rangle \langle \mathbf{r}|$, where $h_{\mathbf{r}} \in [-W, W]$, the expression for the effective disorder strength becomes

$$\lambda = \sqrt{\varphi(\delta V_F^2)} = \alpha(\tau) \frac{W}{\sqrt{3}} + O(W^2), \quad (\text{S.59})$$

where we used that the disorder is uncorrelated at different lattice sites giving $\sum_{\mathbf{r}, \mathbf{r}'} h_{\mathbf{r}} h_{\mathbf{r}'} = \frac{W^2}{3} \delta_{\mathbf{r}, \mathbf{r}'}$. The parameter $\alpha(\tau)$ has the form

$$\alpha(\tau) = 1 + \tau^2 \Delta(V_\tau), \quad V_\tau = V - \frac{\tau}{6} [V, H_0] + O(\tau^2) \quad (\text{S.60})$$

where $\Delta(V_\tau) = \sum_{\mathbf{r}} \left(\langle \mathbf{r} | V_\tau | \mathbf{r} \rangle^2 - \langle \mathbf{r} | V_\tau^2 | \mathbf{r} \rangle \right)$. If in addition the applied periodic field is local, $\Delta(V) = 0$, the finite frequency have forth order corrections in period, $\alpha(\tau) = 1 + O(\tau^4)$. More general result can be obtained for arbitrary period τ using the expansion over small disorder strength,

$$e^{-i(H_1 + \delta V)\tau/2} = e^{-iH_1\tau/2} \left(1 - i\hat{F}_1 \delta V \right) + O(\delta V^2), \quad e^{-i(H_2 + \delta V)\tau/2} = \left(1 - i\hat{F}_2 \delta V \right) e^{-iH_2\tau/2} + O(\delta V^2) \quad (\text{S.61})$$

where we define the superoperator

$$\hat{F}_i = \frac{1 - e^{-\hat{G}_{H_i}}}{\hat{G}_{H_i}} = \sum_k \frac{(-1)^k}{(k+1)!} \hat{G}_{H_i}^k, \quad \hat{G}_H B = i\frac{\tau}{2} [H, B]. \quad (\text{S.62})$$

Then, the Floquet operator for disordered system can be expressed as a perturbed operator for the clean system,

$$U'_F = U_F - \frac{i\tau}{2} e^{-iH_1\tau/2} (\hat{F}_1 \delta V + \hat{F}_2 \delta V) e^{-iH_2\tau/2} + O(\delta V^2) \quad (\text{S.63})$$

The expression for Floquet disorder corrections can be derived from Eq. (S.51) using Taylor expansion we the derivative of the matrix logarithm

$$\frac{d \log A}{dt} = \frac{1}{2\pi i} \int dz \log(z) \frac{1}{z - A} \frac{dA}{dt} \frac{1}{z - A} \quad (\text{S.64})$$

As a result, the expression for Floquet disordered correction in the limit of weak disorder reads

$$\delta V_F = \mathcal{F}\delta V + O(\delta V^2), \quad \text{where} \quad \mathcal{F}\delta V = \frac{1}{4\pi i} \int dz \log(z) \frac{1}{z - U_F} e^{-iH_1\tau/2} (\hat{F}_1 + \hat{F}_2) \delta V e^{-iH_2\tau/2} \frac{1}{z - U_F}. \quad (\text{S.65})$$

This gives us the dependence of α on τ :

$$\alpha(\tau) = \sum_{\mathbf{r}} \sqrt{3\varphi \left((\mathcal{F}|\mathbf{r}\rangle \langle \mathbf{r}|)^2 \right)} \quad (\text{S.66})$$

Eq. (S.59) is valid for static disorder strengths that are smaller than any other relevant energy in static Hamiltonian such as next-neighbour hopping parameter.

If the driving frequency is finite, the series (S.36) can be divergent and δV_F may be essentially different from δV . In particular, in many problems δV is simply a diagonal random matrix. However, low-energy δV_F can have properties of generic random matrix (GRM) as argued in the paper (see for example Fig. 2) and further elaborated on below.

- [1] A. Nica and R. Speicher, *Lectures on the combinatorics of free probability*, Vol. 13 (Cambridge University Press, 2006).
- [2] R. S. James A. Mingo, *Free Probability and Random Matrices* (Springer New York, 2017).
- [3] R. Movassagh and A. Edelman, arXiv preprint arXiv:1710.09400 (2017).
- [4] A. Y. Kitaev, Phys. Usp. **44**, 131 (2001).
- [5] B. A. Bernevig, T. L. Hughes, and S.-C. Zhang, Science **314**, 1757 (2006).
- [6] L. Jiang, T. Kitagawa, J. Alicea, A. R. Akhmerov, D. Pekker, G. Refael, J. I. Cirac, E. Demler, M. D. Lukin, and P. Zoller, Phys. Rev. Lett. **106**, 220402 (2011).
- [7] S. Blanes, F. Casas, J. Oteo, and J. Ros, Phys. Rep. **470**, 151 (2009).
- [8] P. Titum, N. H. Lindner, M. C. Rechtsman, and G. Refael, Phys. Rev. Lett. **114**, 056801 (2015).
- [9] R. Ducatez and F. Huveneers, Ann. Henri Poincaré **18**, 2415 (2017).
- [10] T. A. Loring and M. B. Hastings, Europhys. Lett. **92**, 67004 (2011).
- [11] D. Toniolo, arXiv preprint arXiv:1708.05912 (2017).